ACS APPLIED BIO MATERIALS

www.acsabm.org Article

Carbon Nanotube Fibers for Neural Recording and Stimulation

Noe T. Alvarez,* Elke Buschbeck, Sydney Miller, Anh Duc Le, Vandna K. Gupta, Chethani Ruhunage, Ilya Vilinsky, and Yishan Ma

Cite This: *ACS Appl. Bio Mater.* 2020, 3, 6478–6487 Read Online

ACCESS | Metrics & More | Article Recommendations | Supporting Information

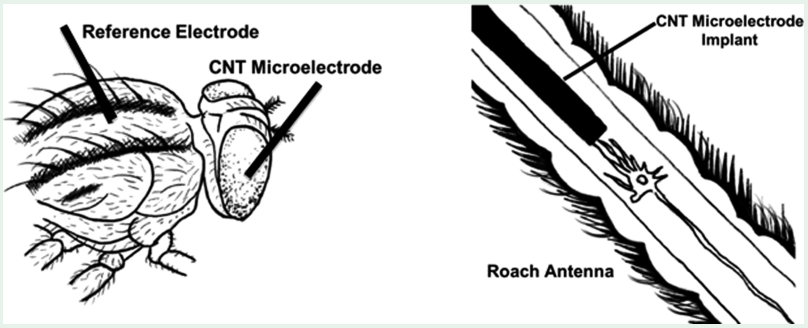

ABSTRACT: Recordings and stimulations of neuronal electrical activity are topics of great interest in neuroscience. Many recording techniques, and even treatment of neurological disorders, can benefit from a microelectrode that is flexible, chemically inert, and electrically conducting and preferentially transfers electrons via capacitive charge injection. Commercial electrodes that currently exist and other electrodes that are being tested with the purpose of facilitating and improving the electron transport between solid materials and biological tissues still have some limitations. This paper discusses carbon nanotube (CNT)-based microelectrodes to record and stimulate neurons and compares their electron transport capabilities to noble metals such as Au and Ag. The recording ability of electrodes is tested through electroretinography on *Sarcophaga bullata* fly eyes by using Au and Ag wires and CNT fibers as electrodes. Stimulation is demonstrated through the implantation of Au wire and CNT fibers into the antennas of the Madagascar hissing cockroach (*Gromphadorhina portentosa*) to control their locomotion. Our results demonstrate that a particular property of the CNT fiber is its high rate of electron transfer, leading to an order of magnitude lower impedance compared to Au and Ag and an impressive 15.09 charge injection capacity. We also established that this carbon nanomaterial assembly performs well for *in vivo* electrophysiology, rendering it a promising prospect for neurophysiological applications.

KEYWORDS: *carbon nanotubes, recording, stimulation, biobots, neuroscience*

INTRODUCTION

Microelectrodes suitable for recording extracellular activity of targeted groups of neurons are critical for neuroscience research and related clinical applications, as it has the ability to stimulate neurons in a targeted fashion. An ideal microelectrode for stimulation should be in intimate contact with neurons and facilitate charge delivery from solid electrodes to soft tissues via capacitive charge transfer. The flow of charged species creates a potential difference at the neuron interface which is the source of the stimulation.[1,2] Basically, during neural stimulation, a useful microelectrode needs to stimulate the neural tissues ideally without generating faradaic electron transfer. In general, neural stimulation requires electrodes that can deliver charges without electrolyzing solvent present near tissues, typically H_2O.[2−4] On the contrary, electrons must maintain signal-to-noise ratio throughout lifetime of the electrode during neural recording.[5] These critical requirements imposed by the method have promoted the search of innovative electrode materials that display larger charge injection capacity (CIC).[6,7]

Improved materials for electrodes have many possible applications and putative advantages. For example, the possibility of effectively communicating man-made devices and the nervous system allows connecting and treating brain diseases by better targeting neural prosthesis based on electrical recording and/or stimulation. Neurological disorders have become the second largest cause of death in 2016, and they were the leading cause of measured disability-adjusted life years.[8] They account for the 7% of the global burden of diseases.[9] The increase of brain-related diseases in the society

Received: July 14, 2020
Accepted: August 18, 2020
Published: August 19, 2020

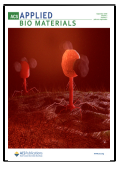

https://dx.doi.org/10.1021/acsabm.0c00861
ACS Appl. Bio Mater. 2020, 3, 6478–6487

has triggered multiple initiatives across the globe that are focused on diagnostics, treatments, and restoration of body functions.[10,11] Neural prosthetic devices include long-term implantations into the nervous system to bypass and/or restore sensory-motor or cognitive functions. Such devices have enormous clinical potential. More specifically, some neural interface systems that already exist can restore loss of functional movement, re-innervate target locations for bladder control, and be used for the treatment of neurological conditions such as epilepsy[12] and Parkinson's disease.[13,14] In general, suitable electrodes require chemical inertness, reduced inflammatory responses, biocompatibility, reduced size, flexibility, and tissue-like hardness with sufficient conductivity or superior electrical characteristics.[2,5,15]

Ideally, the development of innovative electrode materials with potential applications in neuroscience is tested in vertebrates.[16,17] However, testing materials in invertebrates can have its own advantages such as providing a higher throughput, developmental speed, lower costs, and limited regulation allowing researchers quicker and inexpensive characterizations. In fact, there are multiple insect and worm species such as drosophila and *Caenorhabditis elegans* that have shown significant advantages in developmental and molecular neuroscience.[18] Accessibility and quick turnaround are particularly important in studying carbon nanotube (CNT) assemblies (filaments, threads, and fibers) as electrodes because of the additional characteristics related to their nanoscale nature and often-questioned cytotoxicity. *Sarcophaga bullata* fly and Madagascar hissing cockroach (*Gromphadorhina portentosa*), employed here, are insect species that are readily available and have been used extensively in anatomy learning and research.[19−21] Roaches are equipped with multiple sensory cells on their antennas, and they are largely guided for turning and climbing.[22,23] Despite of issues related to organ dimensions of insects, similarly to vertebrates, insects in general rely on vision, audio, touch, smell, and taste for their survival. Most importantly, they possess simpler neural system that can often simulate a neural system of vertebrates, making an ideal model to study stimulations and recordings.

Among extracellular recording methods, the electroretinogram (ERG) is a simple technique that assesses electrical responses to light stimulation of photoreceptors in the retina and underlying interneurons.[24−27] Recorded photoreceptor field potentials, ERGs, are complex signals that in both vertebrates and insects consist of multiple components. In flies, it consist of a sustained component of photoreceptor cells (which in insects are a type of neuron) and relatively sharp transient components that are generated by the activity of downstream interneurons.[24] As light stimulation starts, there is an initial, in the extracellular recording typically positive, voltage-spike "on-transient" that reflects the activation of first order interneurons (laminar neurons), which are the synaptic targets of the photoreceptors R1−R6. This is followed by a sustained electronegative response of the photoreceptors that typically is relatively maintained for the duration of the light stimulus. Upon termination, there tends to be an electronegative "off-transient" that again is thought to result from the lamina. Traditionally, ERG recordings from the surface of the insect eye use a metal-based electrode (usually silver) that is submerged in a saline solution (such as 0.9% NaCl) together with a cotton wick that is placed onto the retinal surface.[24] However, advantages of carbon-based electrodes have been noted, and recently, a graphene film has been employed as a transparent soft electrode material for ERG recordings, with multiple advantages compared to traditional ERG electrodes.[28]

In regards to the electrode design, it is critical that any electrode material has an effective interface with its surrounding medium and efficiently conducts currents so that all components of the signal are adequately captured. ERGs include fast transients because they are fast-producing signals that could be lost or truncated if the temporal properties of the electrode were inadequate. Having fast-responding electrodes that accurately record even high frequency pulses is important to accurately capture neural signals, including those involved in mechanisms underlying diseases related to vision. For example, the genetically important model system *Drosophila melanogaster* is frequently used to study the mechanism of specific neural diseases. For this, researchers typically look for alterations in the components of ERGs,[29,30] which could be distorted if the relatively high-frequency components are not properly captured. Another application is the study of the impact of toxins. For example, ERGs were assessed to study the impact of bis(2-ethylhexyl)phthalate—the most common plasticizer—on proper photoreceptor functioning.[31] Specifically, here, researchers looked at the magnitudes of on-transient and off-transient sizes, as well as photoreceptor depolarization.

In addition to the need for better noninvasive recording electrodes, there is also a need for implantable neural microelectrodes to stimulate neurons. Most such electrodes available today differ from each other based on their material composition, shape, size, and implantation characteristics.[32] Electrode types can be traced to three historical microelectrode technologies: metal microwires, thin-film planar probes employing silicon or polymer substances, or bulk micromachined arrays. Because most of these electrodes are made from stiff metals, a major deficiency is their lack of biocompatibility and foreign nature to the body.[33] The abrupt interface between hard metals and soft brain tissues chronically causes injury that limits the success of current approaches.[33,34] In addition, scar tissue formation prevents effective integration of metal electrodes with surrounding neural tissues, which currently represents a major roadblock for neuroengineering.[35,36] The nature of chronic implants, regardless of their location, requires that such neural implants remain stable throughout the lifespan of the user, usually for many years. It therefore is essential that such materials are chemically inert and have mechanical match in flexibility, in order to be accepted by the human body.[37,38] The search for stable, long-lasting electrodes that elicit little or no deleterious responses in nervous tissues continues.[39]

Most of metal-based microelectrodes such as Au, Pt, and Pt/Ir metals and alloys lack flexibility, and despite being extremely good electrical conductors, they express high impedance and low CIC.[40] Most of the metal electrodes normally have low surface area that limits their CIC values below 0.26 mC/cm^2. Increasing the surface area of metals through surface treatment such as roughening, nanoporosity induction, and other cleaver approaches has been a topic of heavy research in the past decade.[41] Si-based microelectrodes have become quite popular, but most recently, carbon-based ones have been gaining attention.[16,39,40,42] Specifically graphene-based microwires for electrophysiology have shown promising results as an alternative to metals,[40,43,44] but the use of CNTs has also been reported in neurophysiological recordings and stimulations.[17,45−49] CNTs and graphene have shown CICs of 6.5 and

https://dx.doi.org/10.1021/acsabm.0c00861
ACS Appl. Bio Mater. 2020, 3, 6478−6487

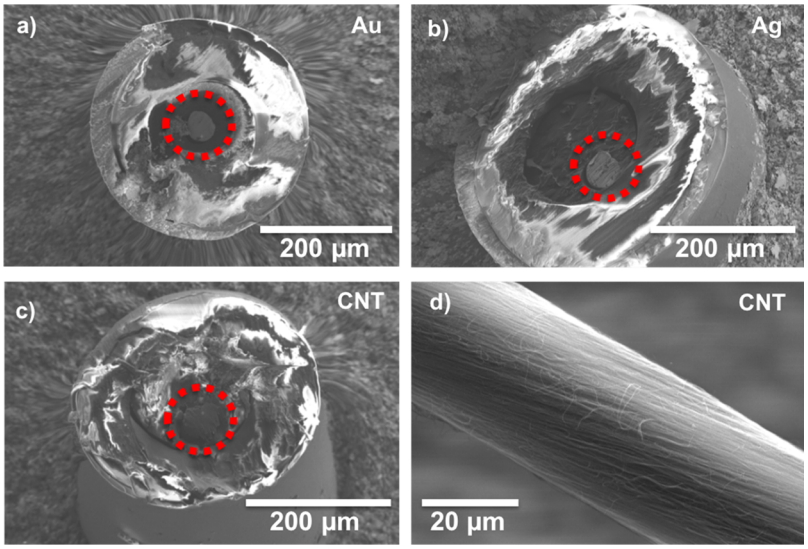

Figure 1. SEM image of microelectrode cross sections employed for ERG recording, circled in red. The conductive core of the microelectrodes are of similar diameter and are embedded within the polymer. Electrode cross sections are (a) Au, (b) Ag, and (c) CNT cross section of polymer-coated CNT fibers. (d) Typical sample of as-spun CNT fiber with ~27 μm diamater.

10.34 mC/cm^2, respectively.[17,40] Their main advantage seems related to their larger potential window of application, larger CIC compared to metals, and higher flexibility compared to carbon fibers.

The exceptional intrinsic physical properties of CNTs offer unique opportunities in multiple extraordinary technological applications.[50] CNTs are conjugated covalently bonding structures; therefore, they are chemically resistant under a broad potential range, which makes them ideal materials for long-term stable microelectrodes.[16,51,52] Because CNTs are nanomaterials, reliable methods of assembly into fibers and handable microelectrodes are important. Unlike industrially produced carbon fibers with well determined specification, CNT fibers are still produced at laboratories; therefore, their assembly methods may induce variations on their performance and characteristics.[16,17,52] Today, there are multiple CNT fiber assembly methods: liquid phase, direct chemical vapor deposition, and dry-spinning from vertically aligned CNTs;[53−56] however, only few methods preserve the pristine properties of CNTs and have the purity required for biomedical applications. Dry-spinning here is most promising because it directly synthesizes spinnable CNT arrays that are free of catalyst. These arrays have the ability to assemble themselves into a continuous ribbon and can be spun into a fiber by a simple twisting and drawing.[53,56,57] The CNTs are relatively soft and flexible and can be spun to a fiber with a diameter from 10 to hundreds of microns diameters without the need of additional chemical treatment. Approximately, each millimeter of CNT arrays allows drawing a meter long CNT ribbon,[58] and the ribbons can be collected at linear speed as high as 16 m/s.[53] In addition, because of their nanoscale dimensions, CNTs in fiber format have a substantially larger area than metal electrodes. Other fiber assembly processes have Fe or other metal catalyst nanoparticles within their structure that can reach over 20% in weight in some cases[59] and likely would cause toxicity if used as microelectrodes.

In this study, we demonstrate dry-spun CNT microelectrodes for acute neuronal activity recording and stimulation. Impedance and CIC were determined for CNT microelectrodes on their cross section. We tested microelectrodes in the framework of ERG recordings, where we contrasted their performance to those of silver and gold electrodes. Specifically, recordings were performed at the cross sections of CNT fibers using ERGs on *S. bullata* eyes. Finally, we tested electrodes in a stimulation paradigm by implanting CNT wire into the antennae of *G. portentosa*, which allowed us to elicit a behavioral response.

EXPERIMENTAL SECTION

CNT Wire Fabrication. CNTs were grown in a vertically aligned forest, and they have the ability to assemble themselves into fibers. Their synthesis process employs Fe/Co as catalyst and C_2H_4 as the carbon source.[53,57] These type of CNTs are known as drawable or spinnable CNTs, and they have the same length, narrow diameter distribution and are also free of catalyst. Assembling fibers of different diameters through this method is simple, and it is accomplished by changing the number of CNTs supplied during assembly, as in prior work reported elsewhere.[53,57] Two sets of CNT fiber were employed during the course of our experiments, 53.46 ± 1.64 μm for recording and 88.47 ± 3.41 μm for stimulation. Diameter measurements were performed using 1000× magnification digitally enhanced microscope, Keyence VHX Series, on 20 sections of fibers. For ERG microelectrode applications (recording), the CNT fibers were encapsulated within a high density polyethylene (HDPE) tubing in order to isolate their periphery from the surrounding media and provide necessary rigidity to apply the electrodes to the fly-eye surface. CNT fibers were inserted within HDPE tubing, and they were heated close to their melting point to completely encapsulate the CNT fiber. The assembly then was cut in order to obtain a clean surface, exposing only the cross sections shown in Figure 1a−c. The exposed ends of the cylindrical Ag, Au wires, and CNT fibers were connected to a metal contact using a Ag paste. Figure 1a−c shows cross sections of such microelectrodes made of Au, Ag, and CNTs that have polymer coating except the cross section of the electrodes. Prior to encapsulation, CNT fibers were densified in acetone for 30 min. Other methods of polymer encapsulation have already been published elsewhere by our group.[60] Figure 1d displays a scanning electron microscopy (SEM) micrograph of the as-spun CNT fiber that shows the surface uniformity of the microelectrodes. Additionally, Figure S1 in Supporting Information has pictures of Au, Ag, and CNT microelectrode cross sections at 1000× magnification for comparison. For the stimulation experiments, the same wires but larger diameter CNT fibers were employed, but unlike in recording, the insertion part

https://dx.doi.org/10.1021/acsabm.0c00861
ACS Appl. Bio Mater. 2020, 3, 6478−6487

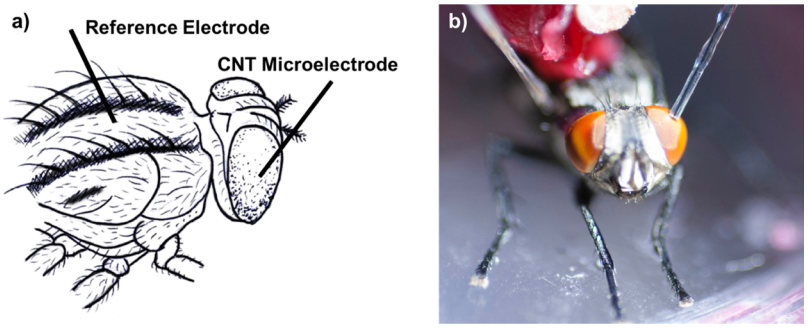

Figure 2. ERG experimental setup: (a) schematic diagram of a *S. bullata* with electrodes connected to the eye and thorax and (b) image of *S. bullata* with CNT microelectrodes contacting the eye.

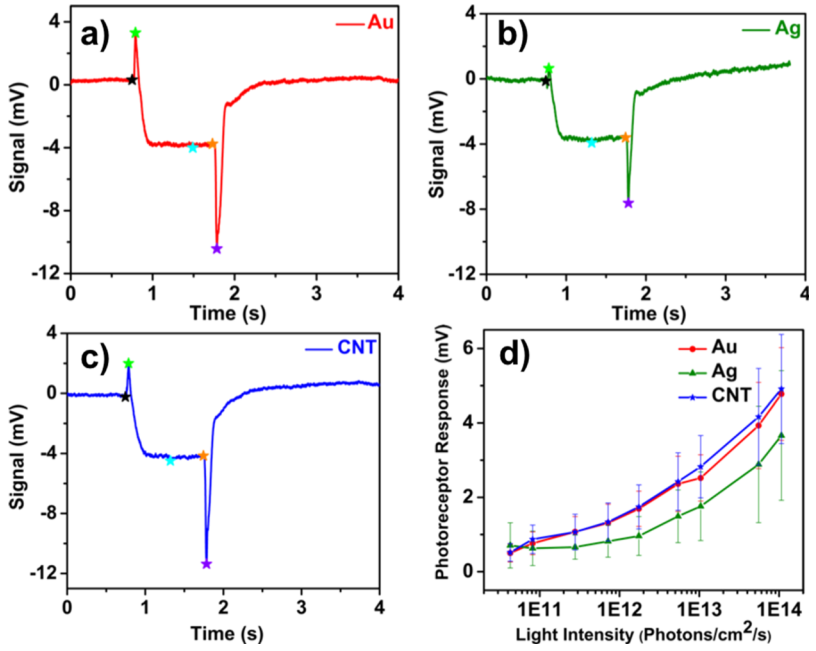

Figure 3. ERG recordings on *S. bullata* eyes. (a) Using CNT electrodes, (b) using gold electrodes, and (c) using silver electrodes, in responses to 490 nm, 1 s light pulse at 1.07×10^{14} photons/cm^2/s (d) response vs log light intensity (V log I) curves from CNT, silver and gold electrodes. At each light intensity, the plotted response is averaged from responses to three light pulses (1 s on, 10 s off) of 490 nm light for all 30 flies. The vertical bars indicate STDEV; $p < 0.05$ for comparisons between gold and silver. No statistical difference between gold and CNT based on *t*-tests. $n = 10$ animals each.

of the electrodes was not coated, instead a bare ∼10 mm length was introduced within the antenna.

Physical and Electrical Characterization. Field emission SEM (FE-SEM) micrographs were recorded using a FEI XL30 at 5−15 kV acceleration voltage to visualize the cross-section surface morphology. The Raman spectra CNT fiber were collected using a Renishaw inVia Raman microscope, Ar-ion laser with an excitation wavelength of 514 nm, Gloucestershire UK.

The electrochemical impedance spectroscopy (EIS) and voltage transient (VT) measurements were performed on CNT fibers and Au and Ag electrodes using a Gamry Reference 600 potentiostat in phosphate buffer saline solution with pH 7.4 at room temperature. For this measurement, three electrode configurations were used with an Ag/AgCl electrode as a reference, Pt wire as a counter, and Au, Ag, and CNT cross sections, respectively, as working electrodes. Impedance was measured at an open circuit potential to the Ag/AgCl electrode. An alternating potential with a 10 mV amplitude was applied in the frequency range from 1 Hz to 100 kHz on Au, Ag, and CNT fiber microelectrodes. Echem Analyst from Gamry was used to analyze the impedance spectra. All electrochemical measurements were performed in a Faraday cage. For water window, cyclic voltammetry was performed between −2.0 and +2.0 V for Au, Ag, and CNT fiber. For the VT measurement, the biphasic, cathode first, and current with pulse width 1 ms with equal amplitude per each phase were delivered. The input current was increased from 100 to 300 μA at which the polarization voltage was observed the maximum (V_p) negative value ∼ −0.9 V for CNT fibers.

Physiological Recordings. To test electrodes in a physiological framework, ERGs were recorded from fly eyes, capturing the response of photoreceptor neurons and interneurons as field potentials of the eye.[24−26,61] ERGs were recorded with Au, Ag, and CNT electrodes (53.46 ± 1.64 μM in diameter) that were placed on the eye (recording) and the thorax of the insect (reference). Commercial conductive paste (Ten20 Conductive, D. O. Weaver and Co.) was used to create contact between the electrodes and the surface of the eye and thorax. Schematics of the experimental design are shown in Figure 2a, and a picture of the insect with the CNT electrode contacting the insect eye can be seen in Figure 2b. A set of 10 recording experiments were collected for Au, Ag, and CNT fiber microelectrodes for a total of 30 flies. Each fly was only used once and with one type of electrode (either Au, Ag or CNT). The quality of the recordings was compared across electrodes. For light stimulation, a 490 nm LED (Roithner Lasertechnick, Vienna, Austria) connected to an optic fiber cable (DigiKey, part# FB143-500-ND) was placed

https://dx.doi.org/10.1021/acsabm.0c00861
ACS Appl. Bio Mater. 2020, 3, 6478−6487

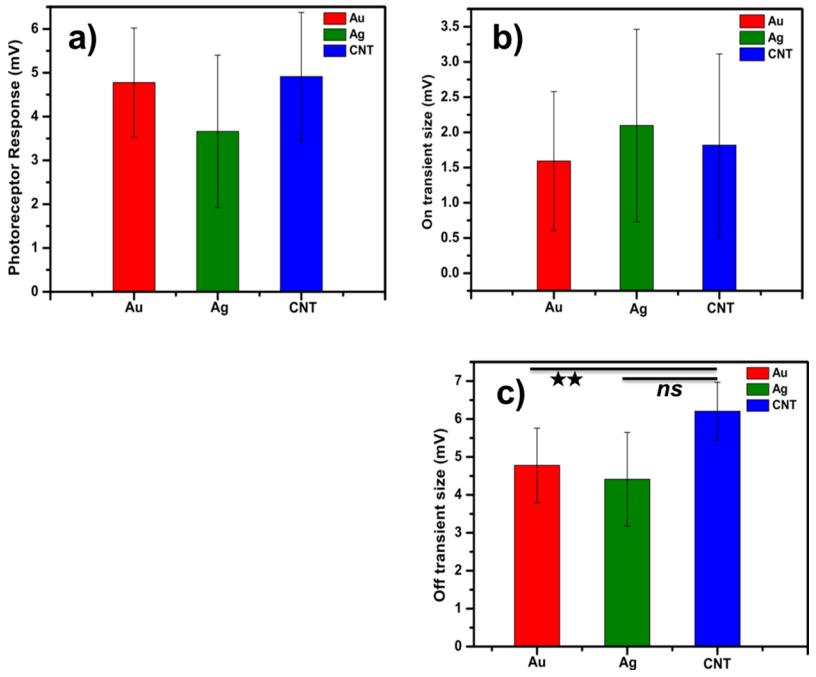

Figure 4. Quantification of ERG responses to light at 1.07×10^{14} photons/cm^2/s from CNT, gold and silver electrodes. (a) Sustained photoreceptor responses: *t*-tests between groups report no statistical difference (p-value > 0.05), ANOVA single-factor reports p-value > 0.05. (b) On-transients: *t*-tests between groups report no statistical difference (p-value > 0.05), ANOVA single-factor reports p-value > 0.05. (c) Off-transients: double-asterisk (**) indicates $p < 0.005$ in *t*-test between CNT and silver; groups that do not share the same letter are statistically different according to a post-hoc Tukey–Kramer test. All responses are averaged from 3 × 1 s on −10 s off pulses. STDEV bars are shown, $n = 10$ animals each.

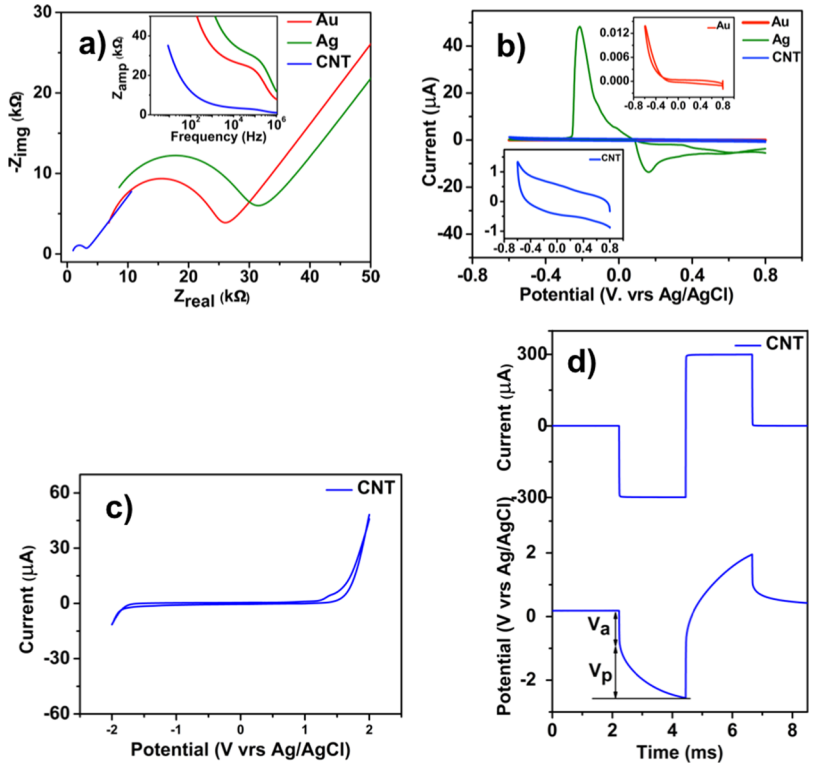

Figure 5. Electron/charge transfer characteristics of the Au, Ag, and CNT electrodes, (a) EIS, Nyquist and Bode (inset) plots, (b) cyclic voltammetry for potential between the 0.8 and −0.6 V. Insets correspond to Au and CNT at different current scales, (c) cyclic voltammogram recorded by sweeping the potential between the voltage limits of −2 to 2 V (vs Ag/AgCl electrode) to determine the water window that limits the water oxidation and reduction voltages. A steep increase in the resistive current is observed; therefore, the water window of CNT fibers ranges from −1.7 to 1.7 V, and (d) CIC for CNT microelectrodes at their cross section.

https://dx.doi.org/10.1021/acsabm.0c00861
ACS Appl. Bio Mater. 2020, 3, 6478−6487

adjacently to the eye so that the light intensity at the eye was 1.07×10^{14} photons/cm^2/s. The ERG setup included a Faraday cage, an A-M Systems model 3000 AC/DC differential amplifier (Carlsborg, WA, USA), an iWorx 118 analog-to-digital converter with LabScribe2 software (iWorks Systems, Dover, NH, USA), oscilloscope, and computer. The amplifier was set to DC mode, a low pass of 20 kHz, and a gain of 50. The sampling rate was 10,000 data points/s.

For quantification of ERGs, a lab custom-made MATLAB program (a modified version of the program published by Stowasser et al.)[25] was used to analyze the magnitude of the three main components: on-transient, photoreceptor response, and off-transient. On-transients were measured as the absolute difference between an average of 100 points prior to light stimulation (represented by black asterisks in Figure 3a−c) and the highest potential value following light stimulation (represented by green asterisks in Figure 3a−c). Photoreceptor responses were assessed as the absolute difference between the baseline (black asterisks) and the lowest potential achieved during stimulation (represented by turquoise asterisks in Figure 3a−c). The amplitude of the off-transient is the absolute difference between the potential value immediately prior to light termination (represented by orange asterisks in Figure 3a−c) and the lowest potential value after light termination (represented by purple asterisks in Figure 3a−c). A comparison of the Au, Ag, and CNT microelectrodes response to photoreceptor stimulation is displayed in Figure 3d. The quantification of Au, Ag, and CNT microelectrodes response is shown in Figure 4a−c.

Neurostimulation. The antenna of Madagascar hissing cockroaches (*G. portentosa*) were stimulated with either Au wire or CNT fibers that were implanted following procedures described in Supporting Information (S-2).[62] Similar procedures are described Latif et al.[63] Specifically, antennal nerves were stimulated by currents that were generated by a commercial electronic device for stimulation (RoboRoach Backpack; purchased from BackyardBrains.com, Ann Arbor MI) that was attached to the cockroach and contained a 1.5 V small circuit battery. Instead of the wires that were supplied by the commercial kit, however, Au and CNT electrodes were attached to respective connectors and implanted into the truncated right or left antenna, leading the cockroach to move away from the side of stimulation. A ground electrode made from the same material as the recording electrodes (Au or CNT) was placed in the thorax. Prior to performing the implants, the roaches were sedated completely by placing them on ice. A 150 grit sandpaper was employed to roughen the roach back and easy the epoxy adhesion of the RoboRoach backpack to the roach thorax. Loctite Super Glue Gel Control, a small-diameter needle, a small cauterizer, and dental wax were employed during implants. Please refer to the experimental procedure for CNT implant within roach antenna (S-2) for more details on the surgery and implant of electrodes in the Madagascar hissing cockroach antenna. The RoboRoach backpack can be activated remotely with a phone through an app that is available at BackyardBrains.com. Directional stimulation is performed directly from the cellphone screen app, using the default parameters provided in instructions. To evaluate and compare Au microelectrodes performance in comparison to CNTs, 5 consecutive stimulations were performed with a 20 s rest time between each stimulation. A total of 5 roaches were used for each electrode type, and their positive responses within 10 attempts for each antenna were tabulated and compared.

RESULTS AND DISCUSSION

EIS of the Au, Ag, and CNT fiber microelectrodes and CIC results are shown in Figure 5. Figure 5a is a summary of impedance measurements, Nyquist plots for each electrode material cross section, and inset displaying Bode plots. From EIS measurement, the impedances of Au, Ag, and CNT fiber microelectrodes were obtained 27 ± 0.085, 30 ± 0.137, and ∼3 ± 0.013 kΩ (5.9 MΩ μm^2), respectively. Smaller impedances of CNT fibers compared to Au and Ag microelectrodes were found suggesting that efficient electron transfer between electrode and electrolyte interface for CNT fibers occurs. Figure 5b illustrates a representative cyclic voltammetry measurement for Au, Ag, and CNT fiber microelectrodes at their cross section. This comparison reveals that Au and CNT are the only microelectrodes that are truly inert within this potential range. This is supported by the fact that Ag-oxidation into Ag_2O and AgO is a well documented phenomenon, especially in electrochemistry.[64] In addition, Ag_2O has higher electrical resistivity compared to Ag and AgO that could negatively affect its performance as an electrode.[65,66] The water window for CNTs is considered from −2 to +2 V which is shown in Figure 5c suggesting the absence of faradaic electron transfer. VT measurements were performed to evaluate the maximum positive and negative polarization voltage (V_p) at the interface as well as the maximum charge that can be injected from the electrode to tissues which is called CIC, Figure 5d. Regarding to CNTs, it is worth to mention that impedance and CIC were determined at the cross section of the CNT fibers, which limits the electron transport path to the tips of CNTs and avoids charge transfer from the sides of CNTs. From Figure 5d, we evaluate the access voltage (V_a = −0.8 V) due to the Ohmic resistance of the electrolyte and then followed by a slowly rising polarization voltage (V_p = 0.8 V) which is due to charging of the electrode/electrolyte interface. CIC was calculated at maximum negative polarization potential (V_p = 0.9 V) using the following equation provided by Wang et al.[40]

$$\mathrm{CIC} = I_c \times t_c/\mathrm{GSA}$$

GSA is the geometric surface area, that is, 1962 μm^2 in our case for all Au, Ag, and CNT microelectrodes. The CIC values for Au, Ag, and CNT microelectrodes are measured to be 0.101, 0.061, and ∼15.09 mC/cm2, respectively, and the charge storage capacity for the CNT fiber is measured to be 2163 mC/cm^2. Vitale et al.[17] have already reported similar CIC values for CNT fibers ∼6.5 mC/cm^2 with 1452 μm^2 GSA. The highest CIC measured for CNT fiber microelectrodes is ∼2.3 times larger as compared to the highest CIC reported before[45] and 149 time larger that Au. In addition, reported CIC and impedance measurements are compared to prior values reported in the literature, Table S1 in Supporting Information. Additional CIC measurements of 10 larger diameter electrodes (∼100 μm), employed for stimulation, gave an average of 13.4 mC/cm^2 with 60% of the electrodes over 15.3 mC/cm^2. These findings suggest that CNTs have substantially higher electron transport at their cut ends than do typical metal wires.

ERGs performed using Au, Ag, and CNT electrodes generally showed comparable results, with each of the three electrode types fully capturing all important components of an ERG of the *S. bullata* eye, including the on-transient, photoreceptor response, and off-transient (Figure 3a−c). The response was also evaluated at different strength—specifically, we evaluated the response characteristic against a series of different light intensities, from 4.28×10^{10} to 1.07×10^{14} photons/cm^2/s (Figure S2 in Supporting Information). For all light intensities, comparable values were measured with all three electrode types, with no substantial relative difference among electrodes. Figure 3d illustrates a response series for which the magnitude of the photoreceptor response to each light intensity was assessed, from the dimmest to brightest value. To further investigate our neural recordings, we examined the strongest response (to 1.07×10^{14} photons/cm^2/s) more closely, in regards to the different components of

https://dx.doi.org/10.1021/acsabm.0c00861
ACS Appl. Bio Mater. 2020, 3, 6478−6487

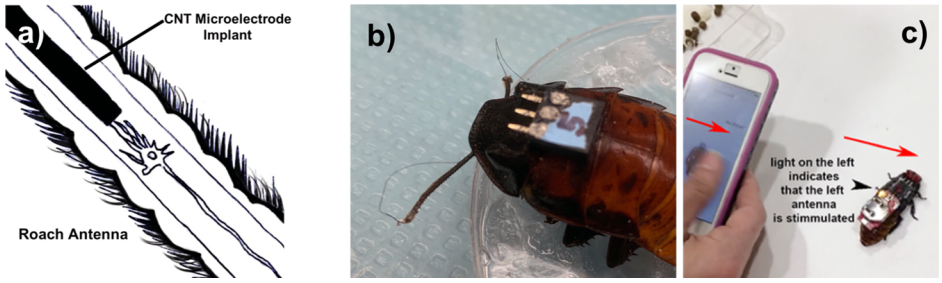

Figure 6. (a) Schematic illustration of electrode insertion into the antenna of a roach and stimulation of mechanosensory neurons of the antenna. (b) Picture of a *G. portentosa* antenna area with CNT electrode implants on its antennas and electrical connectors attached on the roach back. (c) Picture of the roach when wirelessly connected to a cellphone app for stimulation. The roach tends to respond by moving away from the side of stimulation. Stimulation of the left antenna (sweeping to the right as shown in red arrow over phone) triggered a movement of the roach to the right (red arrow above the roach). A full video of CNT electrode elicited behaviors is available in Supporting Information.

the ERG signal. Specifically, we compared the magnitudes of the on-transients, photoreceptor responses, and off-transients from ERGs recorded with CNT electrodes in comparison to those recorded with Ag and Au electrodes. The magnitude of the photoreceptor responses was slightly lower for the Ag-electrode recordings compared to the Au and CNT but not significantly though (Figure 4a). *t*-Tests between groups reported no statistical difference (p-value > 0.05), and analysis of variance (ANOVA) single factor reported p-value > 0.05. Data represented as individual points and their corresponding statistics are shown in Figure S3 of Supporting Information. Our analysis of on-transients (Figure 4b) illustrates comparable values for all three electrodes with no statistical difference between groups, as reported by *t*-tests (p-value > 0.05), ANOVA single factor p-value > 0.05. Analysis of off-transient size reveals that CNT electrodes have similar results as Au electrodes but statistically different from silver electrodes in the direction of having higher magnitude (Figure 4c). Double-asterisk (**) in Figure 4c indicates $p < 0.005$ in *t*-test between CNTs and silver; groups that do not share the same letter are statistically different according to a post-hoc Tukey–Kramer test. Although these differences are more likely an attribute of signal variation of the animals, these findings clearly show that CNT electrodes perform at least as well as the other two electrodes. These findings are in good agreement with other studies that have found carbon-nanomaterial-based electrodes suitable for neural recordings through ERG.[28] It is worth to mention that CNT electrodes record ERG currents as long as the fly is alive. This happens with metal electrodes as well as CNTs suggesting that photoreceptor cells stop responding once insect dies.

For the stimulation experiment, commercial electrodes were replaced by our CNT fiber microelectrodes as implants inside the antennae of the cockroach, thereby stimulating mechanosensory neurons (Figure 6a) that normally signal the roach that it is touching a surface. If the right antenna is successfully stimulated, the roach will then turn toward the left away from that stimulus (to avoid its perceived running into an object) and vice versa. The Video S1 in Supporting Information clearly demonstrates that the roach obeys at stimulation of the left antennae by turning to the right and vice versa. We do not observe any sudden change of direction without stimulation. Roaches tend to heavily rely on their antennae for turning and climbing; in fact, their antennas are equipped with multiple mechano-hygro-receptor cells.[22,23] The information is conveyed from mechanosensory receptors to the central nervous system to alert the roach whenever an object touches the antenna (Figure 6a).[67,68] Using the roach antennal stimulation to test electrodes for their ability to successfully stimulate neurons is relatively easy to set up and provides a reliable and fast readout of the success of the experiment. Figure 6b displays the experimental setup, with one end of the CNT fiber inserted into the truncated roach antenna and the second end connected to a connector into which the battery powered stimulating device can be plugged into. Figure 6c shows the roach fully equipped for stimulation, while it is controlled from an app on a cellphone. Please refer to the Video S1 in Supporting Information to observe the stimulation effects where roaches respond to the stimulations of antennae.

To quantify the response, we compared roaches with Au and CNT fiber electrodes. It is worth to mention that for stimulation experiments, relatively larger CNT fibers (88.47 ± 3.41 μm diameter) were employed to improve the rigidity and easy the insertion/implant process. Typically, larger diameter fibers tend to have larger electrical resistivities,[57] but despite its higher resistance, the electrode performance is comparable to the Au electrodes, as can be seen in Figure 7. As

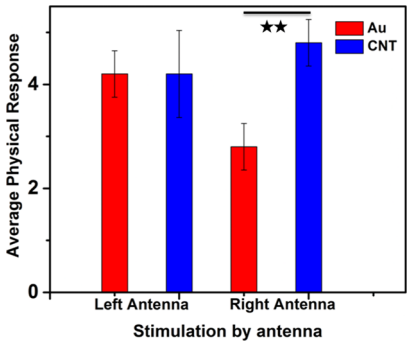

Figure 7. Antennae response following stimulation comparing CNT and Au implantations in the *G. portentosa*. Double asterisk (**) indicates $p < 0.005$ in *t*-test between CNT and Au, making them statistically different according to a post-hoc Tukey–Kramer test. All responses are averaged from 5 × 1 ms on −20 s off stimulation. STDEV bars are shown, $n = 5$ animals for CNT and Au.

can be observed in Figure 7, CNT fibers have higher reproducibility among the stimulations for the right antenna; however, this may be coincidence, as from a biological perspective, no difference between the antennas is expected. Regardless, these results demonstrate that CNT fibers are suitable for the stimulation of the nervous system and clearly more studies are necessary to evaluate closely parameters that

https://dx.doi.org/10.1021/acsabm.0c00861
ACS Appl. Bio Mater. 2020, 3, 6478–6487

determine quantitatively the difference of CNTs with specific microelectrodes of interest. Furthermore, more research is needed to optimize parameters that contribute to variations among the insects, such as depth of the implant, and ultimately long-term viability of such implants.

Taken together, our experiments demonstrate that our nearly contaminant-free fabrication method of CNT fibers leads to a material that like other CNTs are promising for the construction of microelectrodes. CNTs have perfect geometry, small dimensions, and can be assembled into fibers, microcables, and microwires with different diameters starting from a few to hundreds of microns. In contrast to traditional metal- and alloy-based microelectrodes, nanomaterial-based electrodes employs a bottom-up approach that assembles nanosized CNTs into macroscopic fibers and microelectrodes that can be adjusted to application-specific requirements. We attribute this to the dry-spinning CNT fiber assembly method, where basically the number of CNTs incorporated into the assembly can be easily controlled by the width of the CNT array giving a continuous ∼40 m long CNT fibers per batch. CNTs are well known for their electrical conductivity, and electrons can reach ballistic speeds through some of them. They can travel longer distances without scattering, which is the source of electrical resistance for metal wires. Despite these findings, the CNT fibers employed as electrodes have a resistivity of $\sim 1 \times 10^{-5}\ \Omega \times$ m, compared to Au and Ag in the range of $\sim 2 \times 10^{-8}\ \Omega \times$ m, meaning that CNT fibers have about 3 orders of magnitude higher resistivities than Au and Ag microelectrodes.[60] However, it is worth to mention that CNT materials with low electrical conductivity have the ability to performs as well as or better than noble metal electrodes with higher electrical conductivity for this application.[69] These phenomena have been reported before, where carbon-based electrodes have shown lower impedance and higher CIC compared to metals that is consistent with our findings. Most importantly, our physiological recordings demonstrate that despite the lower resistivity, current conduction is sufficient to yield clean and complete physiological recordings. Our data also demonstrates that they outperform Ag and Au electrodes in regards to electron transfer at the interface between the electrode surface and its surrounding material. One major advantage of employing CNT fibers is that their flexibility and their stiffness can be tuned a priori, according to the need of any given experiment. If electrodes were chronically implanted into brain tissues, their potential softness is expected to result in a less damaging probe/tissue interface compared to current approaches. Because of its flexibility, perpetual mechanical trauma that otherwise exists from constant motion between the probe and surrounding tissue[70] likely would be minimized, an approach that warrants further investigation. In addition, fabrication of different sizes of the CNT electrodes has few limitations. Because individual CNTs have single nanometer diameter dimensions, it could be possible to manufacture and employ extremely fine electrodes which still would have substantial surface area to interact with surrounding neurons.

CONCLUSIONS

Over the last decade significant improvements on CNT synthesis, assembly and control over their properties have been demonstrated. This includes the production of CNT fibers that are uniquely assembled without the need of dispersants. Taking advantage of the geometry and physical properties of the nanotubes, these fibers are a promising material for neurophysiological applications. We here explored paradigms that employ insects to test CNT fibers as electrodes and find their performance comparable to those of noble metal wires. Specifically, we used CNT fiber microelectrodes to record the complex extracellular signal of insect photoreceptor neurons and find that both transient and sustained components are captured well, even though the conductivity of the CNT fiber assemblies is substantially lower. Our analysis demonstrates that a particular advantage of CNTs is its high rate of electron transfer, leading to an order of magnitude lower impedance at the interface between solution and the electrode surface. Using the cockroach antennal stimulation paradigm, we also introduced an efficient way to test electrode assemblies in a biological framework. Taken together, our data clearly demonstrate that dry-spun CNT fibers are a suitable material for neural stimulation and recording, and the RoboRoach applied to *G. portentosa* also illustrates that CNT fibers can be successfully implanted. The ability to assemble fibers at different sizes, with exceptionally large surface areas, even for the smallest fibers makes this material particularly promising for neuro−machine interfaces.

ASSOCIATED CONTENT

Supporting Information

The Supporting Information is available free of charge at https://pubs.acs.org/doi/10.1021/acsabm.0c00861.

Neural stimulation video of Madagascar hissing cockroach (MP4)

Pictures of electrodes cross section for comparison, photoreceptor response to two different light intensities, statistical analysis of photoreceptor potential, detailed description of a CNT fiber implant experimental procedure within the antennas, and comparison of literature microelectrode materials (PDF)

AUTHOR INFORMATION

Corresponding Author

Noe T. Alvarez − *Department of Chemistry, University of Cincinnati, Cincinnati, Ohio 45221, United States;* orcid.org/0000-0002-8392-1483; Email: alvarene@ucmail.uc.edu

Authors

Elke Buschbeck − *Department of Biology, University of Cincinnati, Cincinnati, Ohio 45221, United States*

Sydney Miller − *Department of Chemistry, University of Cincinnati, Cincinnati, Ohio 45221, United States*

Anh Duc Le − *Department of Biology, University of Cincinnati, Cincinnati, Ohio 45221, United States*

Vandna K. Gupta − *Department of Chemistry, University of Cincinnati, Cincinnati, Ohio 45221, United States*

Chethani Ruhunage − *Department of Chemistry, University of Cincinnati, Cincinnati, Ohio 45221, United States*

Ilya Vilinsky − *Department of Biology, University of Cincinnati, Cincinnati, Ohio 45221, United States*

Yishan Ma − *Department of Chemistry, University of Cincinnati, Cincinnati, Ohio 45221, United States*

Complete contact information is available at: https://pubs.acs.org/10.1021/acsabm.0c00861

Notes

The authors declare no competing financial interest.

https://dx.doi.org/10.1021/acsabm.0c00861
ACS Appl. Bio Mater. 2020, 3, 6478−6487

■ ACKNOWLEDGMENTS

William Heineman and Pankaj Gupta for insightful discussions. Vesselin Shanov for providing CNT fibers and Annette Stowasser for her assistance with microelectrode fabrication and discussions. This research was supported by a grant from the UCGNI-Neurobiology Research Center Pilot Research Program to N.T.A. and E.B. Support also came from the National Science Foundation under grants IOS-1456757 and IOS-1856341 to E.B.

■ REFERENCES

(1) Pancrazio, J. J.; Deku, F.; Ghazavi, A.; Stiller, A. M.; Rihani, R.; Frewin, C. L.; Varner, V. D.; Gardner, T. J.; Cogan, S. F. Thinking Small: Progress on Microscale Neurostimulation Technology. *Neuromodulation* **2017**, *20*, 745−752.

(2) Cogan, S. F. Neural stimulation and recording electrodes. *Annu. Rev. Biomed. Eng.* **2008**, *10*, 275−309.

(3) Deku, F.; Joshi-Imre, A.; Mertiri, A.; Gardner, T. J.; Cogan, S. F. Electrodeposited Iridium Oxide on Carbon Fiber Ultramicroelectrodes for Neural Recording and Stimulation. *J. Electrochem. Soc.* **2018**, *165*, D375−D380.

(4) Kozai, T. D. Y.; Jaquins-Gerstl, A. S.; Vazquez, A. L.; Michael, A. C.; Cui, X. T. Brain tissue responses to neural implants impact signal sensitivity and intervention strategies. *ACS Chem. Neurosci.* **2015**, *6*, 48−67.

(5) Ward, M. P.; Rajdev, P.; Ellison, C.; Irazoqui, P. P. Toward a comparison of microelectrodes for acute and chronic recordings. *Brain Res.* **2009**, *1282*, 183−200.

(6) Tian, B.; Lieber, C. M. Nanowired Bioelectric Interfaces. *Chem. Rev.* **2019**, *119*, 9136−9152.

(7) Scaini, D.; Ballerini, L. Nanomaterials at the neural interface. *Curr. Opin. Neurobiol.* **2018**, *50*, 50−55.

(8) Feigin, V. L.; Vos, T. Global Burden of Neurological Disorders: From Global Burden of Disease Estimates to Actions. *Neuroepidemiology* **2019**, *52*, 1−2.

(9) Rivnay, J.; Wang, H.; Fenno, L.; Deisseroth, K.; Malliaras, G. G. Next-generation probes, particles, and proteins for neural interfacing. *Sci. Adv.* **2017**, *3*, No. e1601649.

(10) Bargmann, C.; Newsome, W. BRAIN 2015: A Scienctifc Vision. *NIH Working Group Report 2014*; NIH, 2014.

(11) Consortium, H.-P. *The Human-Brain Project*; Report to the European Commission, 2012, Report 2012.

(12) Skarpaas, T. L.; Morrell, M. J. Intracranial stimulation therapy for epilepsy. *Neurotherapeutics* **2009**, *6*, 238−243.

(13) Peña, C.; Bowsher, K.; Costello, A.; De Luca, R.; Doll, S.; Li, K.; Schroeder, M.; Stevens, T. An overview of FDA medical device regulation as it relates to deep brain stimulation devices. *IEEE Trans. Neural Syst. Rehabil. Eng.* **2007**, *15*, 421−424.

(14) Faggiani, E.; Benazzouz, A. Deep brain stimulation of the subthalamic nucleus in Parkinson's disease: From history to the interaction with the monoaminergic systems. *Prog. Neurobiol.* **2017**, *151*, 139−156.

(15) Deku, F.; Cohen, Y.; Joshi-Imre, A.; Kanneganti, A.; Gardner, T. J.; Cogan, S. F. Amorphous silicon carbide ultramicroelectrode arrays for neural stimulation and recording. *J. Neural. Eng.* **2018**, *15*, 016007.

(16) McCallum, G. A.; Sui, X.; Qiu, C.; Marmerstein, J.; Zheng, Y.; Eggers, T. E.; Hu, C.; Dai, L.; Durand, D. M. Chronic interfacing with the autonomic nervous system using carbon nanotube (CNT) yarn electrodes. *Sci. Rep.* **2017**, *7*, 11723.

(17) Vitale, F.; Summerson, S. R.; Aazhang, B.; Kemere, C.; Pasquali, M. Neural stimulation and recording with bidirectional, soft carbon nanotube fiber microelectrodes. *ACS Nano* **2015**, *9*, 4465−4474.

(18) Maximino, C.; Silva, R. X.; da Silva Sde, N.; Rodrigues Ldo, S.; Barbosa, H.; de Carvalho, T. S.; Leao, L. K.; Lima, M. G.; Oliveira, K. R.; Herculano, A. M. Non-mammalian models in behavioral neuroscience: consequences for biological psychiatry. *Front. Behav. Neurosci.* **2015**, *9*, 233.

(19) Heyborne, W. H.; Fast, M.; Goodding, D. D. The Madagascar Hissing Cockroach: A New Model for Learning Insect Anatomy. *Am. Biol. Teach.* **2012**, *74*, 185−189.

(20) Sivasubramanian, P.; Stark, W. S. Photoreceptor properties of an ectopic eye in the fleshfly,Sarcophaga bullata. *Experientia* **1980**, *36*, 993−994.

(21) Gilbert, C.; Strausfeld, N. J. The functional organization of male-specific visual neurons in flies. *J. Comp. Physiol., A* **1991**, *169*, 395−411.

(22) Ritzmann, R. E.; Ridgel, A. L.; Pollack, A. J. Multi-unit recording of antennal mechano-sensitive units in the central complex of the cockroach, Blaberus discoidalis. *J. Comp. Physiol. A Neuroethol. Sens. Neural. Behav. Physiol.* **2008**, *194*, 341−360.

(23) Okada, J.; Toh, Y. Active tactile sensing for localization of objects by the cockroach antenna. *J. Comp. Physiol. A Neuroethol. Sens. Neural. Behav. Physiol.* **2006**, *192*, 715−726.

(24) Vilinsky, I.; Johnson, K. G. Electroretinograms in Drosophila: A robust and genetically accessible electrophysiological system for the undergraduate laboratory. *J. Undergrad. Neurosci. Educ.* **2012**, *11*, A149−A157.

(25) Stowasser, A.; Mohr, S.; Buschbeck, E.; Vilinsky, I. Electrophysiology meets ecology: investigating how vision is tuned to the life style of an animal using electroretinography. *J. Undergrad. Neurosci. Educ.* **2015**, *13*, A234−A243.

(26) Belusic, G. ERG in Drosophila. *Electroretinograms*; Open Access InTech, 2011; pp 221−238.

(27) Bach, M.; Hoffmann, M. B. Update on the pattern electroretinogram in glaucoma. *Optom. Vis. Sci.* **2008**, *85*, 386−395.

(28) Yin, R.; Xu, Z.; Mei, M.; Chen, Z.; Wang, K.; Liu, Y.; Tang, T.; Priydarshi, M. K.; Meng, X.; Zhao, S.; Deng, B.; Peng, H.; Liu, Z.; Duan, X. Soft transparent graphene contact lens electrodes for conformal full-cornea recording of electroretinogram. *Nat. Commun.* **2018**, *9*, 2334.

(29) Himmelberg, M. M.; West, R. J. H.; Elliott, C. J. H.; Wade, A. R. Abnormal visual gain control and excitotoxicity in early-onset Parkinson's disease Drosophila models. *J. Neurophysiol.* **2018**, *119*, 957−970.

(30) Stark, W. S.; Harris, W. A.; Walker, J. A. Genetic dissection of the photoreceptor system in the compound eye of Drosophila melanogaster. *J. Physiol.* **1976**, *256*, 415−439.

(31) Chen, M.-Y.; Liu, H.-P.; Liu, C.-H.; Cheng, J.; Chang, M.-S.; Chiang, S.-Y.; Liao, W.-P.; Lin, W.-Y. DEHP toxicity on vision, neuromuscular junction, and courtship behaviors of Drosophila. *Environ. Pollut.* **2018**, *243*, 1558−1567.

(32) Gunasekera, B.; Saxena, T.; Bellamkonda, R.; Karumbaiah, L. Intracortical recording interfaces: current challenges to chronic recording function. *ACS Chem. Neurosci.* **2015**, *6*, 68−83.

(33) Cheung, K. C. Implantable microscale neural interfaces. *Biomed. Microdevices* **2007**, *9*, 923−938.

(34) Woeppel, K.; Yang, Q.; Cui, X. T. Recent Advances in Neural Electrode-Tissue Interfaces. *Curr. Opin. Biomed. Eng.* **2017**, *4*, 21−31.

(35) Grill, W. M.; Norman, S. E.; Bellamkonda, R. V. Implanted neural interfaces: biochallenges and engineered solutions. *Annu. Rev. Biomed. Eng.* **2009**, *11*, 1−24.

(36) Kolarcik, C. L.; Bourbeau, D.; Azemi, E.; Rost, E.; Zhang, L.; Lagenaur, C. F.; Weber, D. J.; Cui, X. T. In vivo effects of L1 coating on inflammation and neuronal health at the electrode−tissue interface in rat spinal cord and dorsal root ganglion. *Acta Biomater.* **2012**, *8*, 3561−3575.

(37) Thompson, C. H.; Riggins, T. A. E.; Patel, P. R.; Chestek, C. A.; Li, W.; Purcell, E. Toward guiding principles for the design of biologically-integrated electrodes for the central nervous system. *J. Neural. Eng.* **2020**, *17*, 021001.

(38) Wellman, S. M.; Eles, J. R.; Ludwig, K. A.; Seymour, J. P.; Michelson, N. J.; McFadden, W. E.; Vazquez, A. L.; Kozai, T. D. Y. A Materials Roadmap to Functional Neural Interface Design. *Adv. Funct. Mater.* **2018**, *28*, 1701269.

https://dx.doi.org/10.1021/acsabm.0c00861
ACS Appl. Bio Mater. 2020, 3, 6478−6487

(39) Kozai, T. D. Y.; Langhals, N. B.; Patel, P. R.; Deng, X.; Zhang, H.; Smith, K. L.; Lahann, J.; Kotov, N. A.; Kipke, D. R. Ultrasmall implantable composite microelectrodes with bioactive surfaces for chronic neural interfaces. *Nat. Mater.* **2012**, *11*, 1065−1073.
(40) Wang, K.; Frewin, C. L.; Esrafilzadeh, D.; Yu, C.; Wang, C.; Pancrazio, J. J.; Romero-Ortega, M.; Jalili, R.; Wallace, G. High-Performance Graphene-Fiber-Based Neural Recording Microelectrodes. *Adv. Mater.* **2019**, *31*, No. e1805867.
(41) Kim, Y. H.; Kim, G. H.; Kim, A. Y.; Han, Y. H.; Chung, M.-A.; Jung, S.-D. In vitro extracellular recording and stimulation performance of nanoporous gold-modified multi-electrode arrays. *J. Neural. Eng.* **2015**, *12*, 066029.
(42) Welle, E. J.; Patel, P. R.; Woods, J. E.; Petrossians, A.; Della Valle, E.; Vega-Medina, A.; Richie, J. M.; Cai, D.; Weiland, J. D.; Chestek, C. A. Ultra-small carbon fiber electrode recording site optimization and improved in vivo chronic recording yield. *J. Neural. Eng.* **2020**, *17*, 026037.
(43) Lu, Y.; Lyu, H.; Richardson, A. G.; Lucas, T. H.; Kuzum, D. Flexible Neural Electrode Array Based-on Porous Graphene for Cortical Microstimulation and Sensing. *Sci. Rep.* **2016**, *6*, 33526.
(44) Kuzum, D.; Takano, H.; Shim, E.; Reed, J. C.; Juul, H.; Richardson, A. G.; de Vries, J.; Bink, H.; Dichter, M. A.; Lucas, T. H.; Coulter, D. A.; Cubukcu, E.; Litt, B. Transparent and flexible low noise graphene electrodes for simultaneous electrophysiology and neuroimaging. *Nat. Commun.* **2014**, *5*, 5259.
(45) Wang, K.; Fishman, H. A.; Dai, H.; Harris, J. S. Neural stimulation with a carbon nanotube microelectrode array. *Nano Lett.* **2006**, *6*, 2043−2048.
(46) Harreither, W.; Trouillon, R.; Poulin, P.; Neri, W.; Ewing, A. G.; Safina, G. Carbon nanotube fiber microelectrodes show a higher resistance to dopamine fouling. *Anal. Chem.* **2013**, *85*, 7447−7453.
(47) Wang, J.; Deo, R. P.; Poulin, P.; Mangey, M. Carbon nanotube fiber microelectrodes. *J. Am. Chem. Soc.* **2003**, *125*, 14706−14707.
(48) Bosi, S.; Fabbro, A.; Cantarutti, C.; Mihajlovic, M.; Ballerini, L.; Prato, M. Carbon based substrates for interfacing neurons: Comparing pristine with functionalized carbon nanotubes effects on cultured neuronal networks. *Carbon* **2016**, *97*, 87−91.
(49) Tsang, W. M.; Stone, A. L.; Otten, D.; Aldworth, Z. N.; Daniel, T. L.; Hildebrand, J. G.; Levine, R. B.; Voldman, J. Insect-machine interface: a carbon nanotube-enhanced flexible neural probe. *J. Neurosci. Methods* **2012**, *204*, 355−365.
(50) Pugno, N. M. On the strength of the carbon nanotube-based space elevator cable: from nanomechanics to megamechanics. *J. Phys.: Condens. Matter* **2006**, *18*, S1971−S1990.
(51) Janas, D.; Vilatela, A. C.; Koziol, K. K. K. Performance of carbon nanotubes wires in extreme conditions. *Carbon* **2013**, *62*, 438−446.
(52) Yu, X.; Su, J. Y.; Guo, J. Y.; Zhang, X. H.; Li, R. H.; Chai, X. Y.; Chen, Y.; Zhang, D. G.; Wang, J. G.; Sui, X. H.; Durand, D. M. Spatiotemporal characteristics of neural activity in tibial nerves with carbon nanotube yarn electrodes. *J. Neurosci. Methods* **2019**, *328*, 108450.
(53) Alvarez, N. T.; Miller, P.; Haase, M.; Kienzle, N.; Zhang, L.; Schulz, M. J.; Shanov, V. Carbon nanotube assembly at near-industrial natural-fiber spinning rates. *Carbon* **2015**, *86*, 350−357.
(54) Behabtu, N.; Young, C. C.; Tsentalovich, D. E.; Kleinerman, O.; Wang, X.; Ma, A. W. K.; Bengio, E. A.; ter Waarbeek, R. F.; de Jong, J. J.; Hoogerwerf, R. E.; Fairchild, S. B.; Ferguson, J. B.; Maruyama, B.; Kono, J.; Talmon, Y.; Cohen, Y.; Otto, M. J. Strong, light, multifunctional fibers of carbon nanotubes with ultrahigh conductivity. *Science* **2013**, *339*, 182−186.
(55) Koziol, K.; Vilatela, J.; Moisala, A.; Motta, M.; Cunniff, P.; Sennett, M.; Windle, A. High-performance carbon nanotube fiber. *Science* **2007**, *318*, 1892−1895.
(56) Bai, Y.; Zhang, R.; Ye, X.; Zhu, Z.; Xie, H.; Shen, B.; Cai, D.; Liu, B.; Zhang, C.; Jia, Z.; Zhang, S.; Li, X.; Wei, F. Carbon nanotube bundles with tensile strength over 80 GPa. *Nat. Nanotechnol.* **2018**, *13*, 589−595.
(57) Alvarez, N. T.; Miller, P.; Haase, M. R.; Lobo, R.; Malik, R.; Shanov, V. Tailoring physical properties of carbon nanotube threads during assembly. *Carbon* **2019**, *144*, 55−62.
(58) Jiang, K.; Wang, J.; Li, Q.; Liu, L.; Liu, C.; Fan, S. Superaligned carbon nanotube arrays, films, and yarns: a road to applications. *Adv. Mater.* **2011**, *23*, 1154−1161.
(59) Xu, Y.-Q.; Peng, H.; Hauge, R. H.; Smalley, R. E. Controlled multistep purification of single-walled carbon nanotubes. *Nano Lett.* **2005**, *5*, 163−168.
(60) Alvarez, N.; Ochmann, T.; Kienzle, N.; Ruff, B.; Haase, M.; Hopkins, T.; Pixley, S.; Mast, D.; Schulz, M.; Shanov, V. Polymer coating of carbon nanotube fibers for electric microcables. *Nanomat* **2014**, *4*, 879−893.
(61) Charlton-Perkins, M. A.; Sendler, E. D.; Buschbeck, E. K.; Cook, T. A. Multifunctional glial support by Semper cells in the Drosophila retina. *PLoS Genet.* **2017**, *13*, No. e1006782.
(62) BackyardBrains.com. Wirelessly control a cyborg cockroach. https://backyardbrains.com/experiments/roboRoachSurgery (accessed Sept 01, 2019).
(63) Latif, T.; Whitmire, E.; Novak, T.; Bozkurt, A. Sound localization sensors for search and rescue Biobots. *IEEE Sensor. J.* **2016**, *16*, 3444−3453.
(64) Zamora-Garcia, I. R.; Alatorre-Ordaz, A.; Ibanez, J. G.; Garcia-Jimenez, M. G.; Nosaka, Y.; Kobayashi, T.; Sugita, S. Thermodynamic and electrochemical study on the mechanism of formation of Ag(OH)4− in alkaline media. *Electrochim. Acta* **2013**, *111*, 268−274.
(65) Jovic, B.; Jovic, V. Electrochemicla formation and characterization of Ag_2O. *J. Serb. Chem. Soc.* **2004**, *69*, 153−166.
(66) Grdeń, M. Impedance study on the capacitance of silver electrode oxidised in alkaline electrolyte. *J. Solid State Electrochem.* **2017**, *21*, 3333−3344.
(67) Harley, C. M.; English, B. A.; Ritzmann, R. E. Characterization of obstacle negotiation behaviors in the cockroach, Blaberus discoidalis. *J. Exp. Biol.* **2009**, *212*, 1463−1476.
(68) Okada, J.; Toh, Y. The role of antennal hair plates in object-guided tactile orientation of the cockroach (Periplaneta americana). *J. Comp. Physiol., A* **2000**, *186*, 849−857.
(69) Alvarez, N. T.; Ruff, B.; Haase, M.; Malik, R.; Kienzle, N.; Mast, D.; Schulz, M.; Shanov, V. Carbon nanotube fiber spinning, densification, doping and coating for microcable manufacturing. *WSEAS Proccedings: Recent Advances in Circuits, Communications and Signal Processing* 2013; pp 336−341.
(70) Gilletti, A.; Muthuswamy, J. Brain micromotion around implants in the rodent somatosensory cortex. *J. Neural. Eng.* **2006**, *3*, 189−195.

https://dx.doi.org/10.1021/acsabm.0c00861
ACS Appl. Bio Mater. 2020, 3, 6478−6487